A Polymeric Binary Titanium(IV) Sulfide and Its Conversion to Molecular Lewis Base Adducts

Atul K. Verma, Jun-Hong Chou, and Thomas B. Rauchfuss*

School of Chemical Sciences, University of Illinois at Urbana-Champaign, Urbana, Illinois 61801

Received May 19, 1998

Introduction

Much interest has been shown in the development of new routes to transition metal sulfides including solvatothermal approaches,[1] solid-state metathesis,[2] MOCVD,[3] atomic level mixing,[4] and donor solvent assisted reactions of the elements.[5] New methods for the synthesis of binary metal sulfides are of interest because the reaction $M + S_8$ can be difficult to control. Such reactions are highly exothermic (e.g., $\Delta H_f°$ (TiS_2) = ∼−342 kJ/mol)[6] but are characterized by high activation energies. Chianelli and Dines circumvented this difficulty through the reaction of $TiCl_4$ with Li_2S, which affords amorphous TiS_2 admixed with LiCl, the latter being removed by careful solvent extraction.[7] We now disclose a related route that produces a sulfur-rich form of titanium sulfide that is quasimolecular, i.e., extractable into donor solvents.[8] No other titanium sulfide, indeed any metal sulfide, is directly extractable into organic solvents.

The sulfiding agent we employ is ZnS_6(TMEDA), which is easily prepared on a multigram scale via the TMEDA-mediated reaction of Zn and elemental sulfur (TMEDA is *N*,*N*,*N*′,*N*′-tetramethylethylenediamine).[9] We previously showed that ZnS_6(TMEDA) reacts with Cp_2TiCl_2 to give Cp_2TiS_5.[10] The ready formation of titanocene pentasulfide, itself considered a good sulfur transfer agent,[11] demonstrates that the zinc compound is a potent source of S_x^{2-}. Encouraged by this finding, we examined the reaction of ZnS_6(TMEDA) with $TiCl_4$ itself.

Results

Solutions of $TiCl_4$ and ZnS_6(TMEDA) (2.5 equiv) react rapidly in CH_2Cl_2 solution as evidenced by the formation of a brown precipitate. The solid was washed with CH_2Cl_2 to remove the byproduct $ZnCl_2$(TMEDA) and unreacted ZnS_6-(TMEDA). The CH_2Cl_2-insoluble fraction has the formula TiS_x, the chief contaminant being a small amount of TMEDA, as indicated by the fact that the total C, H, N content is less than 4%. Solid TiS_x coprecipitates with ∼25 wt % of elemental sulfur which can be removed either by extraction with CS_2 or by vacuum sublimation at 80−100 °C. After such treatment, the residue was examined by scanning electron microscopy, which showed no sign of crystallinity. In situ X-ray fluorescence analysis (EDX) indicated compositional homogeneity with a Ti:S ratio of ∼1:9.

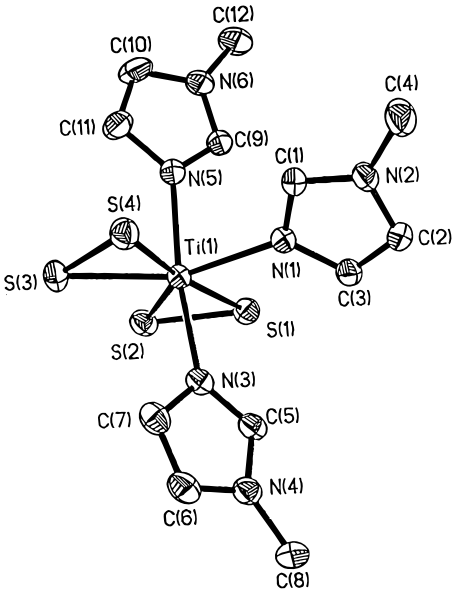

Figure 1. Structure of $TiS_4(MeIm)_3$ with thermal ellipsoids set at 50% probability level.

The key property of TiS_x is its solubility in donor solvents such as pyridine (py) and 1-methylimidazole (MeIm). Extraction into these solvents gave deep blue solutions (λ_{max} ∼ 666 nm) (eq 1). Dilution of pyridine and *t*-Bupy extracts with Et_2O

$$TiCl_4 \xrightarrow[-\ ZnCl_2(TMEDA),\ S_8]{+\ ZnS_6(TMEDA)} TiS_x \xrightarrow[-\ S_8]{L} L_nTi(S_2)_2 \qquad (1)$$

afforded analytically pure samples of TiS_4L_2 (L = py, *t*-BuC_5H_4N). In contrast, precipitation from MeIm extracts produced good yields of blue-black crystals of $TiS_4(MeIm)_3$ (**1**). The difference in the stoichiometry of the pyridine and imidazole adducts is consistent with the smaller steric profile of the imidazole ligand.[12] While it was possible to obtain pure samples of the two pyridine adducts, the MeIm adduct was not obtained in analytical purity, perhaps due to the loss of some MeIm.

Crystallographic characterization of $TiS_4(MeIm)_3$ reveals a structure of idealized C_{2v} symmetry with two coplanar η^2-S_2 groups and three meridional MeIm ligands (Figure 1). This geometry[13] allows the π-donor orbitals on the two persulfido ligands to interact with two different d-π orbitals on Ti. In contrast to **1**, all previously described titanium sulfido and

(1) Sheldrick, W. S.; Wachhold, M. *Angew. Chem., Int. Ed. Engl.* **1997**, *36*, 206; *Angew. Chem.* **1997**, *109*, 214.
(2) Gillan, E. G.; Kaner, R. B. *Chem. Mater.* **1996**, *8*, 333.
(3) Winter, C. H.; Lewkebandara, T. S.; Proscia, J. W.; Rheingold, A. L. *Inorg. Chem.* **1993**, *32*, 3807.
(4) Noh, M.; Johnson, C. D.; Hornbostel, M. D.; Thiel, J.; Johnson, D. C. *Chem. Mater.* **1996**, *8*, 1625.
(5) Ramli, E.; Rauchfuss, T. B.; Stern, C. L. *J. Am. Chem. Soc.* **1990**, *112*, 4043.
(6) Karapet'yants, M. Kh.; Karapet'yants, M. L. *Thermodynamic Constants of Inorganic and Organic Compounds*; Schmorak, J., Trans.; Ann Arbor−Humphrey: Ann Arbor, MI, 1970. Chase, M. W., Jr.; Davies, C. A.; Downey, J. R., Jr.; Frurip, D. J.; McDonald, R. A.; Syverud, A. N. *J. Phys. Chem. Ref. Data Suppl. 1* **1985**, *14*, 1.
(7) $TiCl_4 + Li_2S$: Chianelli, R. R.; Dines, M. B. *Inorg. Chem.* **1978**, *17*, 2758. For related studies, see for H_2S + $Ti(OR)_4$: Sriram, M. A.; Kumta, P. N. *J. Am. Ceram. Soc.* **1994**, *77*, 1381. For $(Me_3Si)_2S$ or $(tert\text{-}Bu)_2S_x$ + $TiCl_4$ (elevated temperatures): Chang, H. S. W.; Schleich, D. M. *J. Solid State Chem.* **1992**, *100*, 62.
(8) Preliminary measurements suggest that this method can be used to prepare soluble sulfides of vanadium and chromium: Verma, A. K., Ph.D. Dissertation, University of Illinois at Urbana-Champaign, 1996.
(9) Verma, A. K.; Rauchfuss, T. B.; Wilson, S. R. *Inorg. Chem.* **1995**, *34*, 3072.
(10) Verma, A. K.; Rauchfuss, T. B. *Inorg. Chem.* **1995**, *34*, 6199.
(11) Leading references: Steudel, R.; Schumann, O.; Buschmann, J.; Luger, P. *Angew Chem., Int. Ed.* **1998**, *37*, 492; *Angew. Chem.* **1998**, *110*, 515.
(12) Sundberg, R. J.; Martin, R. B. *Chem. Rev.* **1974**, *74*, 471.

10.1021/ic980568x CCC: $15.00
Published on Web 10/15/1998

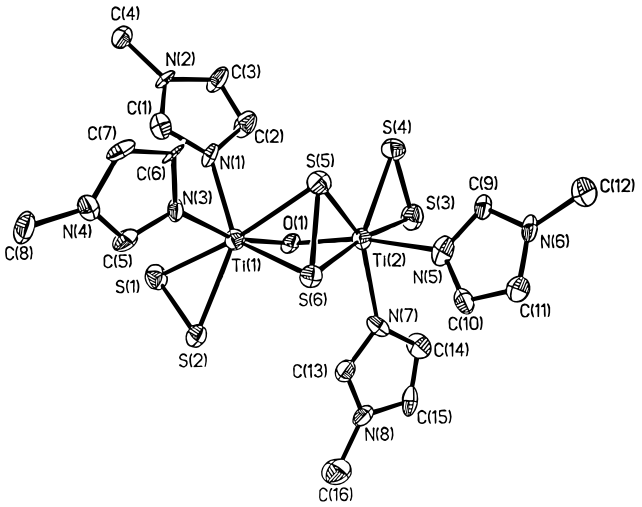

Figure 2. Structure of $Ti_2S_6O(MeIm)_2$ with thermal ellipsoids set at the 50% probability level.

persulfido complexes are stabilized by anionic coligands, e.g., $C_5R_5^-$.[14] In general, there are few examples of neutral metal sulfides that are stabilized only by Lewis bases.[5,9,15]

Samples of $TiS_4(MeIm)_3$ and TiS_x are highly air-sensitive. While the tendency toward hydrolysis was expected, the basis for the oxygen sensitivity was not obvious given that the metal is already in its highest oxidation state and that sulfido ligands are typically not susceptible to oxidation by O_2. Crystallographic analysis shows that the oxygenated product has the formula $Ti_2S_6(O)(MeIm)_4$ (**2**) (eq 2). The two Ti atoms are

$$2Ti(S_2)_2(MeIm)_3 + 0.5\ O_2 \xrightarrow[-\ 2MeIm]{} Ti_2(S_2)_3O(MeIm)_4 + 2\ S \quad (2)$$
$$(\mathbf{2})$$

connected by μ_2-η^2:η^2-S_2 and μ-oxo bridges (Figure 2). Each titanium is also coordinated to one η^2-S_2 as well as two MeIm ligands. The $Ti_2(\mu_2$-η^2:η^2-$S_2)$ unit is very unsymmetrical with the S−S vector twisted at ∼75° relative to the Ti1···Ti2 vector, reflecting the unsymmetrical coordination sphere.[16] The associated Ti−S distances differ by ∼0.15 Å, which is large compared to other $M_2(\mu_2$-η^2:η^2-$S_2)$ complexes. In clusters of the type $Mo_3(\mu_3$-S$)(\mu$-η^2:η^2-$S_2)_3L_6$, the Mo−S (μ_2-η^2:η^2-S_2) distances can differ by as much as 0.1 Å.[17]

(13) Structurally related species include $V(S_2)_2$(terpy) and $Cs_2[Mo(O)(S_2)_2(C_2O_3S)]$: Al-Ani, F. T.; Hughes, D. L.; Pickett, C. J. *J. Chem. Soc., Dalton Trans.* **1988**, 1705. Mennemann, K.; Mattes, R. *J. Chem. Res., M.* **1979**, 102.

(14) $TiSCl_4^{2-}$: Müller, U.; Krug, V. *Angew. Chem., Int. Ed. Engl.* **1988**, *27*, 293; *Angew. Chem.* **1988**, *100*, 277. Krug, V.; Koellner, G.; Müller, U. *Z. Naturforsch.* **1988**, *43B*, 1501. Ti(OEP)S_2: Guilard, R.; Ratti, C.; Tabard, A.; Richard, P.; Dubois, D.; Kadish, K. M. *Inorg. Chem.* **1990**, *29*, 2532. TiS(Me$_4$taa): Housmerikides, C. E.; Ramage, D. L.; Kretz, C. M.; Shontz, J. T.; Pilato, R. S.; Geoffroy, G. L.; Rheingold, A. L.; Haggerty, B. S. *Inorg. Chem.* **1992**, *31*, 4453. Cp*$_2$TiS(py): Sweeney, Z. K.; Polse, J. L.; Andersen, R. A.; Bergman, R. G.; Kubinec, M. G. *J. Am. Chem. Soc.* **1997**, *119*, 4543. $Na_2(THF)_4Cp_2Ti_2S_4$: Lundmark, P. J.; Kubas, G. J.; Scott, B. L. *Organometallics* **1996**, *15*, 3631. Ti(amidinate)$_2$S(py): Hagadorn, J. R.; Arnold, J. *Inorg. Chem.* **1997**, *36*, 2928.

(15) For example: Murphy, V. J.; Parkin, G. *J. Am. Chem. Soc.* **1995**, *117*, 3522.

(16) See $Cp_4TiS_8O_2$: Zank, G. A.; Jones, C. A.; Rauchfuss, T. B.; Rheingold, A. L. *Inorg. Chem.* **1986**, *25*, 1886.

(17) Klingelhofer, P.; Müller, U.; Friebel, C.; Pebler, J. *Z. Anorg. Allg. Chem.* **1986**, *22*, 543. Fedin, V. P.; Müller, A.; Filipek, K.; Rohlfing, R.; Bögge, H.; Virovets, A. V.; Dziegielewski, J. O. *Inorg. Chim. Acta* **1994**, *5*, 223.

Conclusion

A convenient route to a reactive form of titanium sulfide is described. The polysulfidation of $TiCl_4$ affords an extractable—hence the descriptor "quasimolecular"—titanium sulfide. The amorphous and reactive character of this material is consistent with a rapid polymerization after the formation of $Ti(S_n)_2$ (Scheme 1). In contrast, other binary metal sulfides are composed of S^{2-} and S_2^{2-} centers, which, by virtue of their high charge density, strongly bridge metals leading to nonextractable, dense phases. These ideas are summarized in Scheme 1.

Experimental Section

The synthetic operations employed Schlenk techniques and purified solvents. Instrumentation and facilities have been described previously.[9]

Synthesis of TiS_x. A solution of 8.06 g (21.5 mmol) of ZnS_6(TMEDA) in 160 mL of CH_2Cl_2 was treated with 1.4 mL of $TiCl_4$ (12.7 mmol), resulting in the immediate precipitation of a brown solid. After ca. 20 h, the finely divided solid was filtered off (slow) and washed with CH_2Cl_2. Yield: 5.04 g.

Synthesis of $TiS_{\sim 9}$. A sublimation apparatus was charged with 1.02 g of TiS_x and subjected to a static vacuum of 0.1 mmHg at 80 °C. After 96 h, 0.191 g (18 wt %) of yellow solid had collected on the cold probe, leaving 0.809 g of dark brown residue. The sublimate was shown to be elemental sulfur by its solubility in CS_2 and its IR spectrum (ν_{S-S} = 469 cm^{-1}). Semiquantitative microprobe analysis of the compound was performed with Zeiss 960 scanning electron microscope (SEM) equipped wih a energy-dispersive X-ray spectroscopy (EDX) detector. The dark brown powder was mounted on an aluminum stub with conducting carbon tape to avoid charge accumulation on the sample surface under bombardment of the electron beam during measurements. The sample was exposed to the air for about 30 s during the sample preparation. Data acquisitions were performed using an accelerating voltage of 20 kV and a 100 s accumulation time. The Ti:S ratio of 1:9 ratio is the average of seven measurements on different spots of the sample.

$TiS_4(MeIm)_3$. To 3.02 g of TiS_x was added 20 mL of MeIm. The resulting slurry was filtered to remove 0.806 g of elemental sulfur. The dark-blue filtrate was layered with 60 mL of toluene and maintained at 4 °C for 5−7 days to afford blue-black crystals. Yield: 2.23 g (43%). Anal. Calcd for $C_{12}H_{18}N_6S_4Ti$: C, 39.74; H, 4.73; N, 17.94; S, 27.38; Ti, 10.22. Found: C, 38.56; H, 4.94; N, 17.98. IR (KBr): 440, 467, 521 cm^{-1}. UV−vis (MeIm): 390, 666 nm.

$TiS_4(4\text{-}RC_5H_4N)_2$ (R = H, t-Bu). A slurry of 1.0 g of TiS_x in 10−15 mL of pyridine was stirred for ∼30 min. During this time, the slurry changed from dark brown to dark green-blue concomitant with the appearance of a yellow precipitate. The solution was filtered to removed the precipitated sulfur. The dark green-blue filtrate was diluted with ∼100 mL of Et_2O to give a dark green-blue powder. Yield: 0.79 g (86%, assuming TiS_9). The *tert*-butylpyridine adduct was prepared similarly. Anal. Calcd for $C_{10}H_{10}N_2S_4Ti$ (pyridine adduct): C, 35.92; H, 3.01; N, 8.38; S, 38.36; Ti, 14.32. Found: C, 35.47; H, 3.19; N, 8.08. Anal. Calcd for $C_{18}H_{26}N_2S_4Ti$ (*tert*-butylpyridine adduct): C, 48.41; H, 5.89; N, 6.27. Found: C, 48.49; H, 5.87; N, 6.39.

$[Ti_2S_6(O)(MeIm)_4]\cdot MeIm$. A blue solution of 1.02 g of $TiS_4(MeIm)_3$ in ca. 20 mL of MeIm was treated with 8 mL of dry air. The initial dark-blue color of the solution quickly changed to purple. The purple solution was diluted with 50 mL of toluene to afford purple-black crystals. Yield: 0.678 g (78%). Anal. Calcd for $C_{20}H_{30}N_{10}OS_6Ti_2$: C, 33.61; H, 4.23; N, 19.60; S, 26.92; Ti, 13.40. Found: C, 34.36; H, 4.30; N, 19.47; Ti, 13.82. UV−vis (MeIm): 548 nm.

X-ray Structure of $TiS_4(MeIm)_3$. The data crystal was mounted using oil (Paratone-N, Exxon) to a thin glass fiber. The sample was bound by faces (0 1 1), (0 −1 −1), (0 1 −1), (0 −1 1), (1 0 −1), and (−1 0 1). Distances from the crystal center to these facial boundaries were 0.05, 0.05, 0.06, 0.06, 0.18, and 0.18 mm, respectively. Crystal and refinement details are given in Table 1. Systematic conditions suggested the space group $P2_1/n$. Standard intensities monitored during frame collection showed no decay. Intensity data were reduced by

Scheme 1

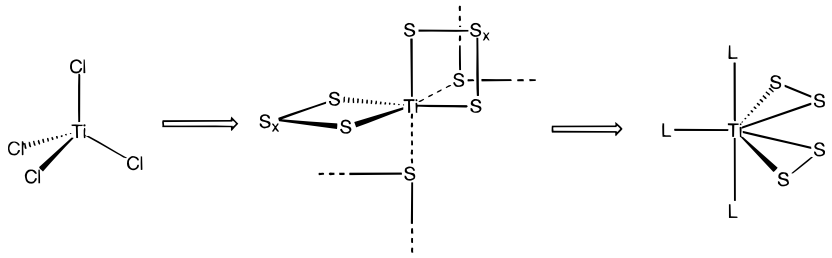

Table 1. Crystallographic Data for $TiS_4(MeIm)_3 \cdot (C_6H_5Me)_{0.5}$ and $[Ti_2S_6(O)(MeIm)_4] \cdot MeIm$

empirical formula	$C_{15.5}H_{22.5}N_6S_4Ti$	$C_{20}H_{30}N_{10}OS_6Ti_2$
fw	468.62	714.70
a, Å	8.9205(1)	8.852(1)
b, Å	10.1979(2)	17.597(3)
c, Å	23.4470(6)	19.766(3)
α, deg	90.00	90.00
β, deg	96.265(2)	99.538(3)
γ, deg	90.00	90.00
T, K	198	198
Z, V, Å^3	4, 2120.24(7)	4, 3036.3(8)
space group	$P2_1/n$ (No. 14)	$P2_1/c$ (No. 14)
ρ_{calcd}, g/cm^3	1.468	1.563
radiation	Mo Kα	Mo Kα
μ, mm^{-1}	0.811	0.973
R_1/wR_2 [a,b] ($F > 4\sigma(F)$)	0.0464/0.0916	0.0981/0.1407
R_1/wR_2 [a,b] (all data)	0.2124/0.1776	0.0927/0.1094

[a] $R_1 = \sum(|F_o| - |F_c|)/\sum|F_o|$ for $F > 4\sigma(F)$. [b] $wR_2 = [\sum[w(F_o^2 - F_c^2)^2]/\sum[w(F_o^2)^2]]^{1/2}$ for $F > 4\sigma(F)$.

3d-profile analysis using SAINT and corrected for Lorentz−polarization effects and for absorption. Scattering factors and anomalous dispersion terms were taken from standard tables.

The structure was solved by direct methods; the correct Ti and S atom position was deduced from an E-map. Subsequent cycles of isotropic least-squares refinements followed by unweighted difference Fourier syntheses revealed positions for the remaining non-H atoms. The *N*-methyl H atoms were disordered with respect to a rotation of the methyl group around N−C bonds. This disorder was treated as an ideal model, where the H atoms were rotated from each other by exactly 60°. Methyl H atom positions, N−CH_3, were optimized by rotation about N−C bonds with idealized C−H, N−H, and H−H distances. Remaining H atoms were included as fixed idealized contributors. Ring and methyl H atom *U*'s were assigned as 1.2 and 1.5 times, respectively, the U_{eq} of adjacent C atoms. One toluene solvate molecule was present at the origin with partial occupancy, which was refined independently to ca. 51%. This toluene molecule was found to be disordered with another molecule related via a symmetry operation defined by $(-x + 2, -y, -z)$. All the non-H atoms, except those in the solvate, were refined with anisotropic thermal coefficients. Successful convergence of the full-matrix least-squares refinement on F^2 was indicated by the maximum shift/error for the last cycle. The highest peaks in the final difference Fourier map were in the vicinity of the Ti and S atoms; the final map had no other significant features. A final analysis of variance between observed and calculated structure factors showed no dependence on amplitude or resolution. Key distances and angles are presented in Table 2.

X-ray Structure of $Ti_2(S_2)_2(\mu_2\text{-}\eta^2\text{:}\eta^2\text{-}S_2)(\mu_2\text{-}O)(MeIm)_4 \cdot MeIm$. The data crystal was mounted using oil (Paratone-N, Exxon) to a thin glass fiber. The sample was bound by faces (0 0 1), (0 0 −1), (0 1 0), (0 −1 0), (1 0 0), and (−1 0 0). Distances from the crystal center to these facial boundaries were 0.005, 0.005, 0.009, 0.009, 0.19, and 0.19 mm, respectively. Crystal and refinement details are given in Table 3. Systematic conditions suggested the unambiguous space group $P2_1/c$. Standard intensities monitored during frame collection showed no decay. Intensity data were reduced by 3d-profile analysis using SAINT and corrected for Lorentz−polarization effects and for absorption.

Table 2. Selected Distances (Å) and Angles (deg) in $TiS_4(MeIm)_3$ (**1**) with Standard Deviations in Parentheses

Ti−S2	2.3484(9)	Ti−S3	2.3635(9)	Ti−S1	2.4055(9)
Ti−S4	2.428(1)	S1−S2	2.061(1)	S3−S4	2.069(1)
Ti−N5	2.196(2)	Ti−N3	2.204(2)	Ti−N1	2.216(2)

N5−Ti−N3	171.63(9)	N5−Ti−S1	91.11(7)
N5−Ti−S2	92.76(7)	N5−Ti−S3	92.98(7)
N5−Ti−S4	89.73(7)	N3−Ti−N1	83.83(9)
N3−Ti−S1	88.99(7)	N3−Ti−S2	93.84(7)
N3−Ti−S3	92.35(7)	N3−Ti−S4	88.59(7)
N1−Ti−S1	84.66(7)	N1−Ti−S2	135.89(7)
N1−Ti−S3	135.68(7)	N1−Ti−S4	84.57(7)
S1−Ti−S4	169.05(4)	S2−Ti−S1	51.36(3)
S2−Ti−S3	88.35(3)	S2−Ti−S4	139.50(4)
S3−Ti−S1	139.65(4)	S3−Ti−S4	51.15(3)

Table 3. Selected Distances (Å) and Angles (deg) of $[Ti_2S_6(O)(MeIm)_4] \cdot MeIm$ (**2**) with Standard Deviations in Parentheses

Ti1−Ti2	3.032(3)	Ti1−S1	2.401(4)	Ti1−S2	2.366(4)
Ti1−S5	2.596(4)	Ti1−S6	2.440(4)	Ti1−N1	2.185(9)
Ti1−N3	2.232(9)	Ti1−O1	1.835(7)	Ti2−S3	2.409(4)
Ti2−S4	2.359(4)	Ti2−S5	2.463(4)	Ti2−S6	2.602(3)
Ti2−N5	2.246(9)	Ti2−N7	2.176(9)	Ti2−O1	1.835(7)
S1−S2	2.068(4)	S3−S4	2.063(5)	S5−S6	2.061(4)

O1−Ti1−N1	89.1(3)	O1−Ti1−N3	163.9(3)
N1−Ti1−N3	82.5(3)	O1−Ti1−S2	103.1(2)
N1−Ti1−S2	137.0(3)	N3−Ti1−S2	92.4(2)
O1−Ti1−S1	100.8(2)	N1−Ti1−S1	86.1(3)
N3−Ti1−S1	92.3(2)	S2−Ti1−S1	51.4(1)
O1−Ti1−S6	86.4(2)	N1−Ti1−S6	135.6(3)
N3−Ti1−S6	90.1(3)	S2−Ti1−S6	86.8(1)
S1−Ti1−S6	138.1(1)	O1−Ti1−S5	81.7(2)
N1−Ti1−S5	87.4(3)	N3−Ti1−S5	84.2(2)
S2−Ti1−S5	134.7(1)	S1−Ti1−S5	172.9(1)
S6−Ti1−S5	48.2(1)	S2−Ti1−Ti2	111.9(1)
S1−Ti1−Ti2	133.0(1)	S5−Ti1−Ti2	51.19(8)
S6−Ti1−Ti2	55.53(9)	Ti−S6−Ti2	73.8(1)
Ti2−S5−Ti1	74.6(1)	Ti−O1−Ti2	111.5(4)

Scattering factors and anomalous dispersion terms were taken from standard tables.

The structure was solved by direct methods by relaxing the cross-term criteria for the negative quartets; the correct Ti and S atom positions were deduced from an E-map. Subsequent cycles of isotropic least-squares refinements followed by an unweighted difference Fourier synthesis revealed positions for the remaining non-H atoms. Methyl H atom positions, N−CH_3, were optimized by rotation about N−C bonds with idealized C−H, N···H, and H···H distances. Remaining H atoms were included as fixed idealized contributors. The ring and methyl H atom *U*'s were assigned as 1.2 and 1.5 times, respectively, the U_{eq} of the adjacent C atoms. Non-H atoms were refined with anisotropic thermal coefficients. Successful convergence of the full-matrix least-squares refinements on F^2 was indicated by the maximum shift/error for the last cycle. The highest peaks in the final difference Fourier map were in the vicinity of the Ti and S atoms; the final map had no other significant features. A final analysis of variance between observed and calculated structure factors showed dependence on amplitude and resolution. Key distances and angles are presented in Table 3.

Acknowledgment. This research was supported by the National Science Foundation. Materials characterization utilized the Center for Microanalysis of Materials located in the Seitz Materials Research Laboratory (DOE contract DEFG02-96ER45439).

Supporting Information Available: An X-ray crystallographic file, in CIF format, for **1** and **2** is availble on the Internet only. Access information is given on any current masthead page.

IC980568X